J Ther Eng, Vol. 7, No. 7, pp. 1614–1627, November, 2021

Journal of Thermal Engineering
Web page info: https://jten.yildiz.edu.tr
DOI: 10.14744/jten.2021.0006

Research Article

Enhancement technique of heat transfer using inserted twisted tape

Prashant R NAWALE[1,*], Atharva A MULE[2], Sudesh B POWAR[1], Pramod P KOTHMIRE[1]

[1]School of Mechanical and Civil Engineering, Maharashtra Institute of Technology Academy of Engineering Alandi(D), Pune, Maharashtra, India 412105
[2]Department of Chemical Engineering, Indian Institute of Technology Roorkee, Haridwar, Uttarakhand, India 247667

ARTICLE INFO

Article history
Received: 08 April 2020
Accepted: 26 July 2020

Key words:
Augmented pipe; CFD analysis; Heat transfer enhancement technique; Twisted tape

ABSTRACT

Enhancements in heat transfer systems are being applied for recovery of heat in domestic as well as industrial applications in many areas. These are done by generating turbulence and swirl motion in the flow by inserting inserts to reduce the thermal resistance of heat transfer. This paper presents the experimental and numerical results of heat transfer enhancement of cooling of a confined space by inserting twisted tape in a pipe buried in concrete under the floor. The Reynolds number is fixed to 15000. Thirteen cases are considered varying the configurations and designs of twisted tapes and the effects of different types of perforations and slots on twisted tapes are studied. Water as the test fluid flowed in pipe inserted with twisted tapes. Heat is transferred from a heating plate to water along the pipe length through concrete to simulate the heat transfer from a room and the water temperature rise is studied. To validate the experimental results, ANSYS-FLUENT is used as the CFD tool with a Standard k-ε turbulence flow model and the SIMPLE algorithm is implemented. Flow physics behaviour is displayed using velocity and temperature profiles inside the pipe. Insertion of twisted tapes shows that the heat transfer is enhanced due to swirling action, friction and turbulence. The experimental differences in inlet and outlet water temperature validated the CFD simulation results. The temperature distribution on a single twisted tape with increasing twist ratio is found to be the most efficient for heat transfer enhancement of the cooling floor surface with a water temperature rise of 1.62 °C along a pipe length of 1.8 m.

Cite this article as: Nawale PR, Mule AA, Powar SB, Kothmire PP. Enhancement technique of heat transfer using inserted twisted tape. J Ther Eng 2021;7(7):1614–1627.

INTRODUCTION

Practically, hydronic systems are used for cooling applications in which the roof and floor surfaces are cooled by flowing cold water through pipes. For the enhancement of heat transfer, inserts are used to extract additional heat from a conditioned space. Swirl flows are generated with the help of twisted tapes as these flows increase turbulence and heat transfer area and thus the rate of heat transfer. Most of the practical applications in industries such as cooling and heating devices, heat exchangers, cyclone separators,

*Corresponding author.
*E-mail address: prashantnawale2011@gmail.com, prnawale@mitaoe.ac.in

This paper was recommended for publication in revised form by Regional Editor Liu Yang

Published by Yıldız Technical University Press, İstanbul, Turkey

agricultural spraying machines, diesel and petrol engines, vortex tubes, gasoline engines, furnaces, etc. use swirl flow generation for improvement in heat transfer.

The twisted tape is one of the best examples of swirl flow generation. The geometrical parameters of twisted tapes are needed to study the design of heating and cooling appliances. Several geometries of various configurations have been analyzed for heat transfer improvement in heating and cooling applications with CFD.

Eiamsa-ard et al. [1] conducted an experiment and a study by changing twist tape parameters such as different twist ratios and free space ratios on the full length and regularly-spaced twisted tapes. At similar conditions, full length twisted tapes offered higher heat transfer rate, friction factor and thermal performance factor than the regularly-spaced ones. Augmented friction factor and heat transfer decreased with increasing space ratio and twist ratio. Regularly spaced twisted tape with greater free space ratio gave considerably lesser heat transfer rate compared to other tapes because of significant decaying of the swirl flows. Maradiya et al. [2] studied different heat transfer improvement techniques by varying construction complexity and geometrical configuration at different thermal and flow conditions. It was concluded that heat transfer enhancement occurs because of an increase in the turbulence intensity, reduction in flow cross-section area and increase in tangential flow. The full-length twisted tape proved to be better than the regularly spaced one.

Tamna et al. [3] analyzed the system of double V-ribbed twisted tapes for heat transfer enhancement. The highest-pressure loss and heat transfer from the inserts of V-ribbed twisted tape is found at the largest relative rib height or blockage ratio. Maakoul et al. [4] studied a 3-dimensional CFD model using the ANSYS-FLUENT software to determine the annulus side fluid flow pressure drop and heat transfer coefficient for various configurations. For validation of numerical results, a comparative study was done with experimental results using empirical correlations to calculate pressure drop and heat transfer characteristics for double pipe heat exchangers with helical baffles. Yongsiri et al. [5] examined the results of a numerical study on heat transfer as well as the turbulent flow in a channel by providing inclined detached-ribs. A numerical study was done to study the effects of inclined detached ribs at different attack angles on frictional factors and thermal performance behaviours at Reynolds number ranging from 4000 to 24,000. Murugesan et al. [6] studied the friction factor characteristics of a circular tube fitted with plain and trapezoidal-cut twisted tapes. They investigated experimental uncertainties of Reynolds number, friction factor and Nusselt number in heat exchanger tube by using ANSI/ASME standard.

Deshmukh et al. [7] used a delta wing vortex generator as an insert in a tube and studied the thermohydraulic characteristics for various geometrical parameters viz. height to inner tube diameter ratio, pitch to projected length ratio (p/pl) and angle of attack for air as the working fluid. Empirical correlations were developed for frictional factor and Nusselt number in terms of other parameters. Promvonge et al. [8] performed an experimental study for investigation of heat transfer and airflow friction characteristics for diagonally fitted 30^o angle-finned tapes in a square duct at different fin pinch to duct height ratios. Air was used as a test fluid with Reynolds number ranging from 4000 to 23,000. Skullong et al. [9] conducted experimental and numerical work based on the heat transfer improvement of square-duct fitted with 30^o oblique horseshoe baffles in a heat exchanger. The technique of heat transfer enhancement used was the reattachment/impingement flow incorporated by longitudinal vortex flows.

Sivashanmugam et al. [10] experimented and studied the thermal performance, friction factor and heat transfer of helical screws of equal and unequal lengths of different twist ratios fitted in circular tubes and observed that for a given twist ratio, the heat transfer enhancement for left-right helical screw insert was higher than that for a straight helical twist. Chang et al. [11] examined the flow interactions and thermal performances between the bursting or/and separated flows developed by 90^o or 45^o grooves/ribs along with wire coils and the tube-core vortices and found that the stable single-cell axial swirls in smooth-coil tubes yield to the unstable multi-cell vortical flows in grooved/ribbed-coil tubes. Skullong et al. [12] performed an experimental study on heat transfer characteristics and turbulent flow in a solar air heater channel attached with combined groove turbulators and wavy-rib. The experiments were conducted by maintaining the airflow rate to obtain Reynolds numbers from 4,000 to 21,000. Bhuiya et al. [13] studied the effect of triple twisted tapes on thermal performance characteristics, efficiency, friction factor, and heat transfer rate. The contained triple twisted tapes improved the friction factor and higher heat transfer rate over the plain tube in the range of 3.85 to 4.2 times more as compared with the plain tube, increasing the thermal performance up to 1.44. Hong et al. [14] did an experimental study on the hydraulic and thermal performances in a plain tube mounted with short length helical tapes. It was found that Nu and frictional factor increase with increasing tape length ratios, decreasing hole diameter ratios and decreasing pitch length ratios.

The above surveys show that analysis of temperature distribution inside the pipe onto the twisted tape using CFD with a single-phase fluid for different augmented cases and configurations of twisted tape was not carried out previously. The present study is based on flow and temperature distribution along with the twisted tape, pipe wall and the thermal conditions of the water inside the pipe. With the help of the CFD simulation tool ANSYS-FLUENT, we have investigated the improvement for an increase in the absorption of heat in order to have a higher cooling effect in a room. We have chosen a confined space and we found that the temperature reduction was 7 °C across the room. We also have co-related one of the twisted tapes with respect to the industrial application of heat exchanger. Though, caution has to be taken on the water inlet conditions and geometrical dimensions of twisted tape.

METHODOLOGY

The pipe pattern shown below is used for analysis of heat removal from a conditioned space. A 3D geometric CATIA V5R20 model having dimensions 1.8m × 0.2m × 0.075m was used for the analysis. The floor surface is made up of concrete for simplification of geometry in ANSYS-FLUENT. A schematic diagram of the conditioned space used for cooling is shown in Figure 1.

The material used for the serpentine pipe pattern shown above is polybutylene [15]. The pipe has an inner diameter of 2 in is buried in concrete below the floor. The total length of the pipe below the floor surface in the construction used in the above geometry is 55 meters and heat transfer enhancement in the confined space is due to the full length of pipe spread below the floor. A small part from the conditioned space has been extracted for the experimental point of view and analysis of this study is based on this part. For our convenience of study, a pipe length of 1.8 meters buried with concrete has been taken, and insulation is provided below the block to study the heat removal of room above the floor. For analysis, full length twisted tape is used for the swirl flow in the pipe.

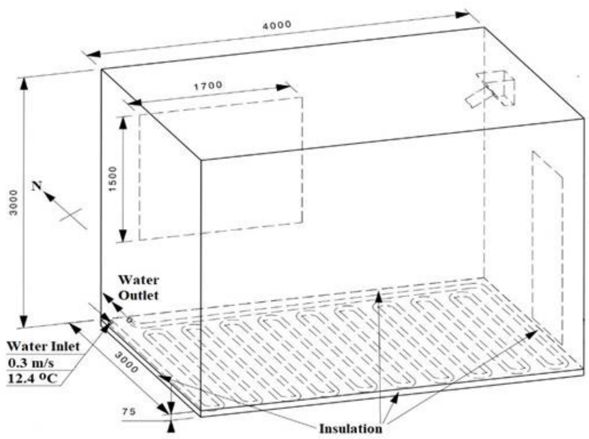

Figure 1. Schematic diagram of conditioned space for cooling.

The schematic diagram shown above is the extracted part from a conditioned space for analysis of cooling below the floor surface and a constant temperature condition of 42 °C has been applied on the upper surface of the concrete block to simulate the experimental study. Figure 2 show the location of the water inlet & outlet and dimensions in millimetres. Below the floor surface, a slab of concrete material, 75mm in thickness is provided insulation beneath it. Water is pumped into the pipe having a cross-sectional area of 1942 mm^2, with a velocity of 0.3 m/s. Symmetrical boundary conditions are used for both sides of the pipe for the continuity of concrete blocks. The distance between the two pipes is 0.2 m; hence two symmetry walls are 0.2 m apart. Full-length inserts are added for heat enhancement by inserting them into the pipe, i.e. the length of twisted tapes is 1.8 m.

The analysis was performed in a pipe section of 1.8 m length with and without inserts. Thirteen such geometries were analysed for the above geometry using the ANSYS-FLUENT software. The ANSYS 16.0 version has been used and simulations were performed in the 3-Dimensional steady state condition. The flow model used was the Turbulence flow model with Standard k-ε model and near wall treatment was used as standard wall function for the simulation setup. The computations are based on the Finite Volume Method (FVM) used extensively in CFD applications. The SIMPLE algorithm, which uses velocity and pressure correlation and enforces mass conservation to obtain the pressure field has been implemented. In meshing, the pipe has been finely meshed for better results. For flexible results of the output, the input water temperatures and

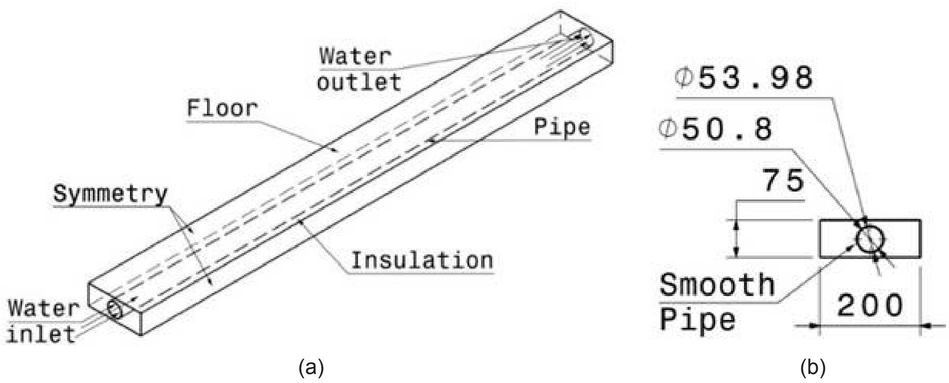

Figure 2. Schematic diagram of (a) isometric and (b) front view of the extracted part for analysis from conditioned space for cooling below the floor surface.

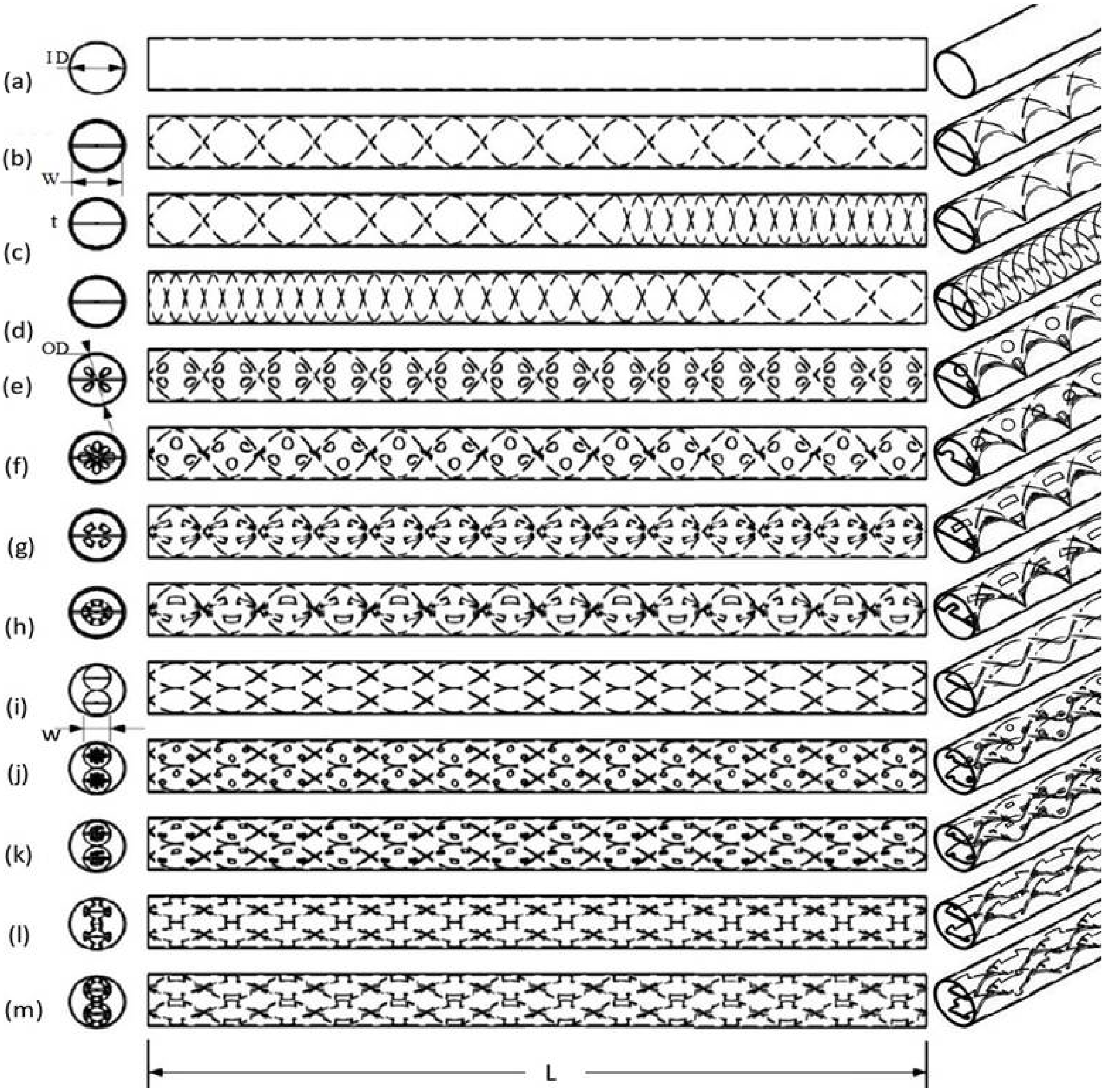

Figure 3. Front, side, and, isometric views of different configurations of twisted tapes for heat enhancement by swirl flow and turbulence, respectively (a) smooth pipe, (b) single twisted tape of constant twist ratio, (c) twisted tape with increasing twist ratio, (d) twisted tape with decreasing twist ratio, (e) parallel circular perforated twisted tape, (f) zigzag circular perforated twisted tape, (g) parallel rectangular perforated twisted tape, (h) zigzag rectangular perforated twisted tape, (i) co-swirl double twisted tapes, (j) double zigzag circular perforated twisted tapes, (k) double zigzag rectangular perforated twisted tape, (l) double parallel slotted twisted tapes, (m) double zigzag slotted twisted tape.

other geometrical parameters were considered almost constant. All isometric views are shown in Figure 3, and these inserts are made such that the surface area of twisted tapes is the same in single twisted tape and double twisted tapes. All the twisted tapes have almost the same surface area. The perforations and slots are given to twisted tape for turbulence generations inside the pipe.

For smooth and augmented twisted tapes, different configuration designs are used to get temperature distribution over the twisted surface. Width and Twist ratio for a single twisted tape is taken as 48 mm and 2.5, respectively and for dual twisted tape is 25 mm and 2.5, respectively so that surface contact area with fluid is the same, which is 0.2 m^2. The thickness of the twisted tape is 2 mm for all augmented cases. Twisted tape with uniform decreasing twist ratio is from 2.5 to 1 and with uniform increasing twist ratio is from 1 to 2.5 from the inlet. Zigzag and parallel circular perforated single twisted tape have circular perforations of diameter 12 mm and zigzag circular perforated double twisted tape have circular perforations of diameter 6 mm. The zigzag rectangular perforated single twisted tape has perforations of 18.42 mm × 6.42 mm, the zigzag rectangular perforated double twisted tape has rectangular perforations of 3.55 mm x 7.09 mm, and zigzag and parallel slots of double twisted tape has slots of dimensions 18.42 mm x 6.42 mm. This study gives numerical data of temperature distribution along the length by considering the surface area of twisted tape as constant. The gap of the inner diameter of the pipe and twisted tape is 1.4 mm for all single twisted tape and 0.4 mm for all double twisted tape.

Experimental Setup and Procedure

The system is installed in a confined space, available for performing experiments. The inlet and outlet temperature differences are studied using various twisted tape configurations and designs. As shown in Figure 4, a concrete block of dimensions 1.8m x 0.2m x 0.75m with a hole of diameter equal to the outer diameter of the polybutylene pipe was set, covering the test pipe. For every run, twisted tapes of various configurations were inserted into the pipe covering the whole pipe length. Insulation was provided at the bottom of the concrete block using spray foam so that all the transferred heat from the confined space should enter the pipe through concrete and no heat loss in any other direction should take place. Thermocouples were inserted into the concrete block touching the pipe wall at distances of 0.1m, 0.5m, 0.9m, 1.3m and 1.7m from the inlet and temperatures were noted at these positions. A heating plate with dimensions 1.8m x 0.2m was used for heating the top surface of concrete block while maintaining a constant temperature of 42°C throughout the heating plate. The inlet water at a constant temperature of 12.4°C was stored in a cold-water tank and was pumped using a pump with a constant mass flow rate and a velocity of 0.3 m/s. Water flows through this pipe and gets heated due to the heat transfer through the concrete. The outlet water temperature was more than the inlet temperature due to the heat gain. This water was collected and stored in a reservoir. A support table was used to support the block. Thirteen experiments were performed corresponding to the thirteen configurations of twisted tapes and temperatures were noted.

Meshing of Geometrical Model

The elements contained in the meshing geometry is of polyhedral cells. For 3-Dimensional modelling, CATIA V5 software was used. A fine mesh was generated on the model with 1017452 cells, 6557825 faces and 5533124 nodes and 3 cell zones, 14 face zones.

ANSYS workbench platform gives fine meshing, as shown in Figure 5. For geometry meshing of surface and volume mesh, ANSYS-FLUENT is used as a solver. The volume mesh shown above is for the concrete zone. The polyhedral mesh pattern is used for this geometry. For smooth and augmented twisted tape, a similar meshing process was used.

A single zigzag circular perforated twisted tape of meshing with polyhedral elements is shown in Figure 6. Similarly, rectangular perforations are applied to the zigzag and parallel rectangular perforated single twisted tape meshed with polyhedral element pattern.

A 3D model with unstructured mesh was generated for all cases. Out of them, the single TT with constant twist ratio for different mesh sizes was checked for temperature difference, as shown in Table 1. The Table shows only a slight increase in the value of temperature difference for an increase of about 100000 cells. The result was such that after increasing the number of cells from coarse to medium, an increase in significant temperature was observed. But, after going from medium to fine meshing, the temperature difference was almost constant. Thus, to reduce the unnecessary processing and computation of FLUENT, a medium size meshing with 1,017,452 cells was used for the present

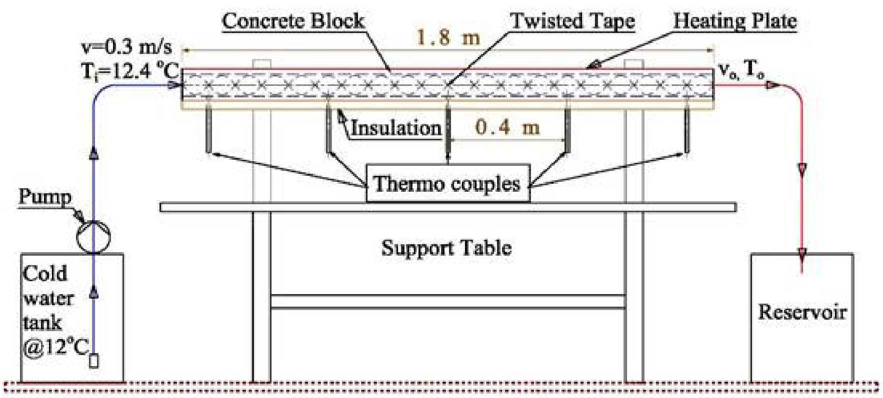

Figure 4. Experimental setup.

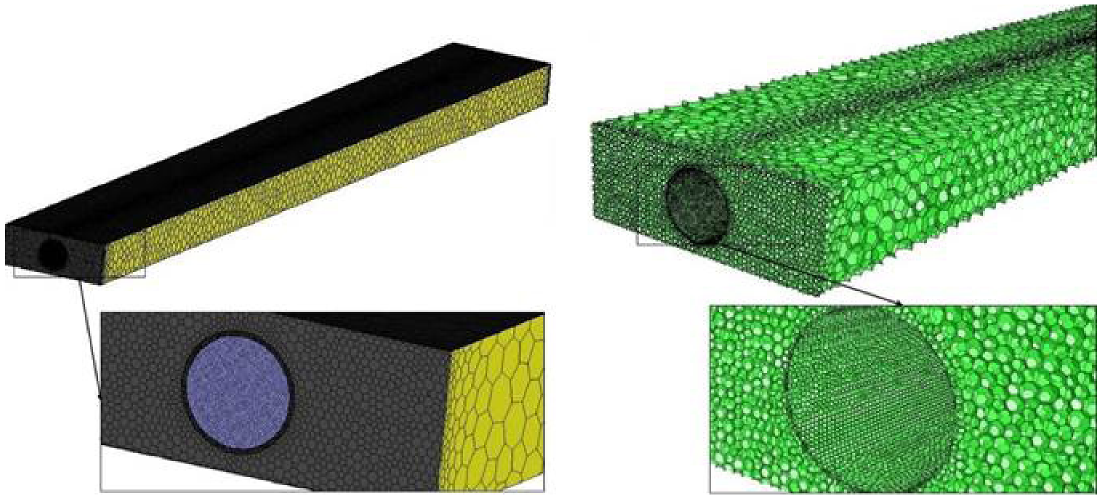

Figure 5. Geometry meshing of (a) surface mesh and (b) volume mesh.

Figure 6. Single zigzag circular perforated twisted tape meshed with polyhedral elements.

Table 1. Grid independency test (Re = 15000, Single TT with constant twist ratio, T_{IN} (°C) = 12.55)

	Total number of cells	T_{out} (°C)	ΔT
MESH 1	817,452	13.56	1.01
MESH 2	908,918	13.57	1.02
MESH 3	1,192,315	13.59	1.04

simulations. Figure 6 shows the change in temperature difference between the inlet and outlet in comparison to number of cells.

Governing Equations and Boundary Conditions

The energy conservation equation for a fluid domain, accounting for volumetric heat release can be written as:

$$u\frac{\partial(\rho_f C_f T_f)}{\partial x}+v\frac{\partial(\rho_f C_f T_f)}{\partial x}+w\frac{\partial(\rho_f C_f T_f)}{\partial x} = k_f\frac{\partial^2 T_f}{\partial x^2}+k_f\frac{\partial^2 T_f}{\partial y^2}+k_f\frac{\partial^2 T_f}{\partial z^2} \quad (1)$$

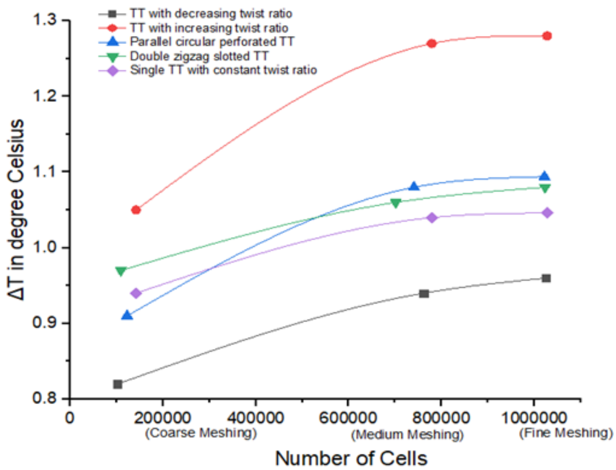

Figure 6. Grid independency test for different TT configurations.

The fluid continuity equation, accounting to flow pattern can be written as:

$$\frac{\partial(\rho_f u_i)}{\partial x_i}=0 \quad (2)$$

The momentum equations in x, y, and z-direction, accounting to momentum change can be written as:

$$\frac{\partial\left(\rho_f u_i u_j\right)}{\partial x_j}=\frac{\partial}{\partial x_j}\left(-\rho_f\overline{u_i' u_j'}\right) +\frac{\partial}{\partial x_j}\left[\mu\left(\frac{\partial u_i}{\partial x_j}+\frac{\partial u_j}{\partial x_i}-\frac{2}{3}\delta_{ij}\frac{\partial \mu_k}{\partial x_k}\right)\right]-\frac{\partial p}{\partial x_i} \quad (3)$$

The concrete, aluminium, and pipe have solid zones created inside the pipe. Four zones occurred in single twisted tape, and five zones occurred in double twisted tape. For the fluid zone, the outlet type is pressure outlet at atmospheric condition and the inlet type is velocity inlet.

The velocity in a range of 0.3 m/s and 0.4 m/s gives a better temperature distribution in the area from water to floor surface [5].

The twisted tape is made up of aluminium, and hence these are solid zones created inside the twisted tape. The pipe surface is coupled to the solid zone and fluid zone. The floor surface and insulation surface are at a constant temperature for calculation of maximum heat removal by inserting twisted tape inside the pipe.

Material Properties

The most appropriate insulation is selected based on its density, specific heat and thermal conductivity. The pipe is made up of polybutylene material.

Table 2. Temperatures in degree Celsius given to boundary surfaces

Boundary	Material	T(°C)
Floor	Concrete	42
Insulation	Insulation	38

Table 3. Materials and their properties

Materials	ρ (kg/m^3)	C_p (j/kgk)	K (w/mk)
Concrete	2400	800	0.6
Insulation	48	790	0.01
Polybutylene	940	1421	0.2741

All the material properties are assigned to the cell zones and face zones for setup in ANSYS-FLUENT software.

CFD Analysis

After calculations are performed by the ANSYS-FLUENT software, the results are taken in the form of contours and vector plots. The colour band shows a better visualization of the figures. The blue colour denotes a low value; it increases up to red colour showing a higher value of temperature. The unit of temperature shown here is degree Celsius. As the top part of the pipe receives heat from the room, it has a higher temperature than the bottom.

The contours of temperature distribution over the pipe surface show that the temperature at the upper surface of the pipe is 30% more than the circumferential sides of the pipe because the temperature of the floor is 5% higher.

The temperature distribution over the twisted tape in the augmented pipe is such that the cold water from the inlet takes heat from the floor surface of the test room and thus increases its temperature along the pipe to the outlet.

The velocity contour shown above in Figure 10 shows the velocity distribution of the flow of water in a swirl motion. We can see that the blue colour corresponding to the surface of the twisted tape has a low value due to the no-slip condition. The temperature increase of the water is enhanced due to the purely swirl motion and turbulence generated by the twisted tape.

The isometric view of contours of temperature distribution in a normal plane shown in Figure 11 gives the distribution of temperature from pipe to twisted tape. The temperature distribution along the flow direction has been shown here. Outer layers have high values compared to the centre as they are close to the pipe. We can see from the figure that very low values are obtained near the twisted

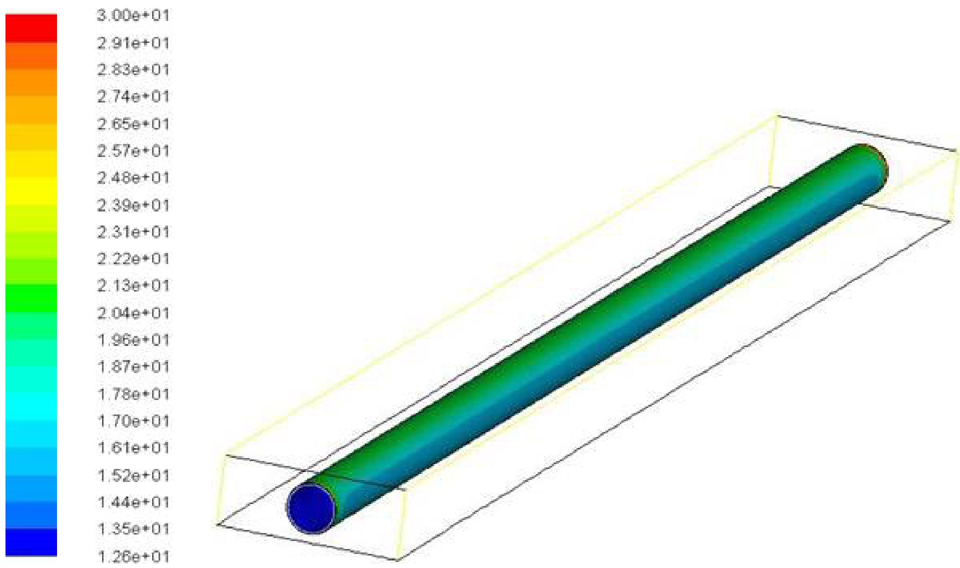

Figure 7. Contours of temperature distribution over the pipe surface.

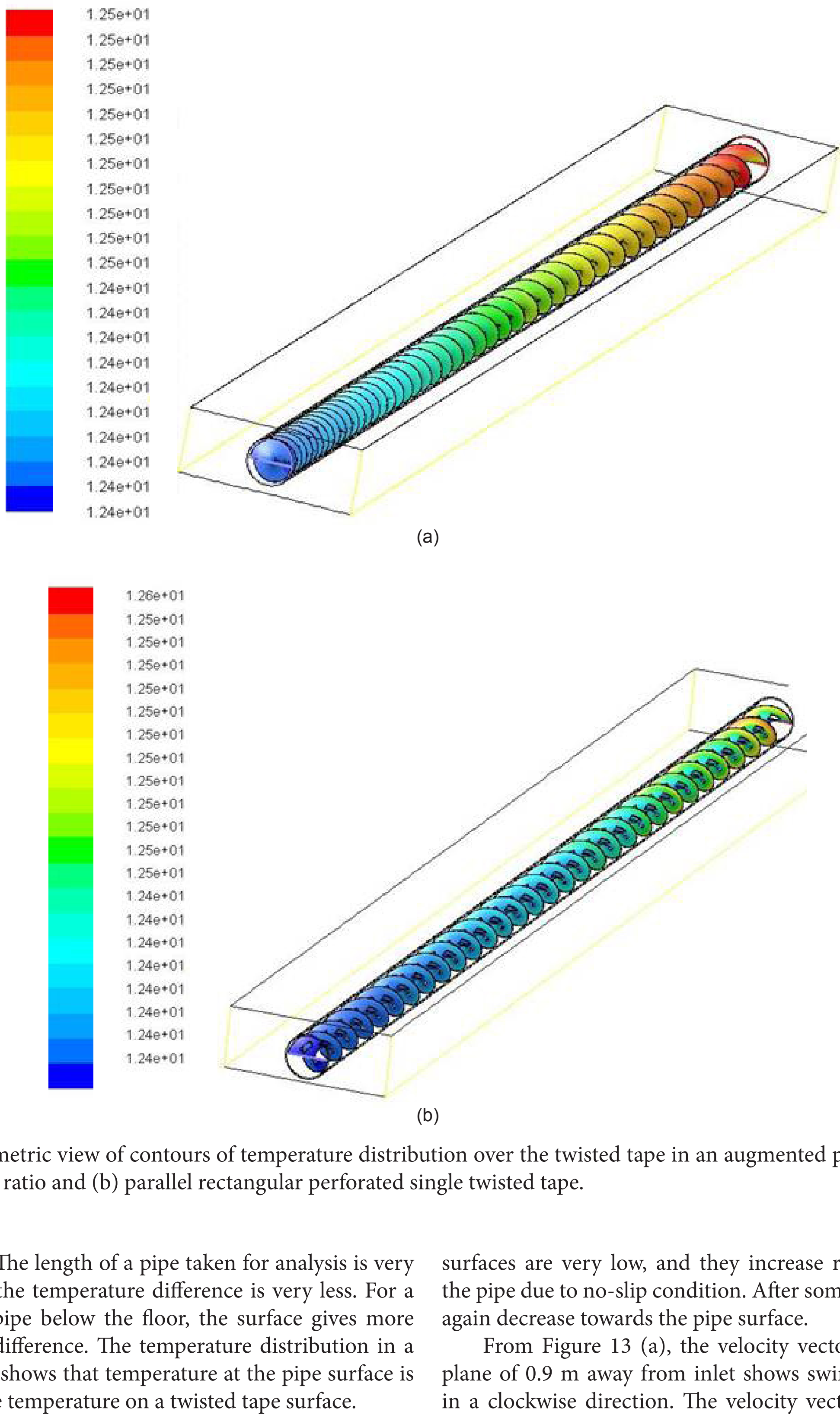

Figure 8. Isometric view of contours of temperature distribution over the twisted tape in an augmented pipe with (a) increasing twist ratio and (b) parallel rectangular perforated single twisted tape.

tape surface. The length of a pipe taken for analysis is very small; hence the temperature difference is very less. For a fully spread pipe below the floor, the surface gives more temperature difference. The temperature distribution in a section plane shows that temperature at the pipe surface is more than the temperature on a twisted tape surface.

The velocity vector plot from Figure 12 shows the distribution of velocity radially and along the length of the pipe. Velocity values near the perforations and twisted tape surfaces are very low, and they increase radially towards the pipe due to no-slip condition. After some distance, they again decrease towards the pipe surface.

From Figure 13 (a), the velocity vector diagram at a plane of 0.9 m away from inlet shows swirl flow of water in a clockwise direction. The velocity vector coloured by velocity magnitude at the middle of the rectangular perforation present in the twisted tape shows the flow of water through the rectangular perforation. From Figure 13 (b),

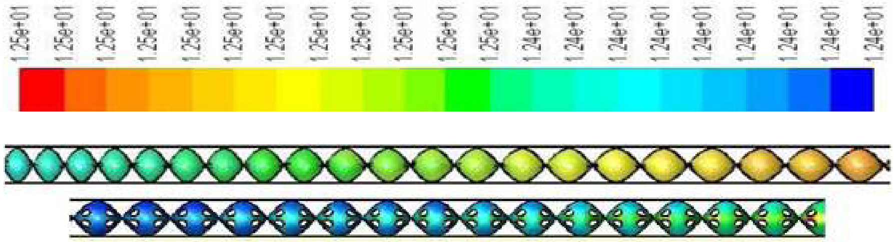

Figure 9. Side view of contours of the temperature distribution over twisted tape in an augmented pipe with increasing twist ratio and parallel circular perforated single twisted tap, respectively.

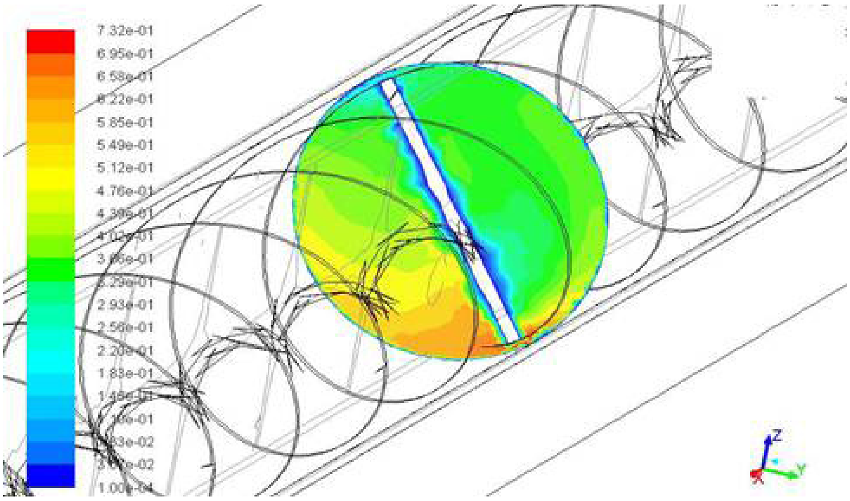

Figure 10. Isometric view of contours of velocity distribution in a normal plane.

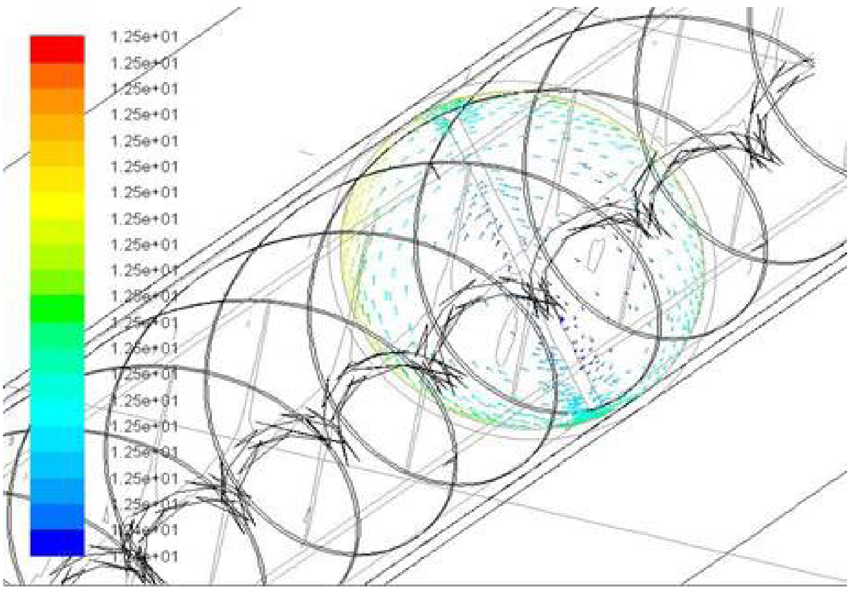

Figure 11. Isometric view of the temperature profile in a normal plane.

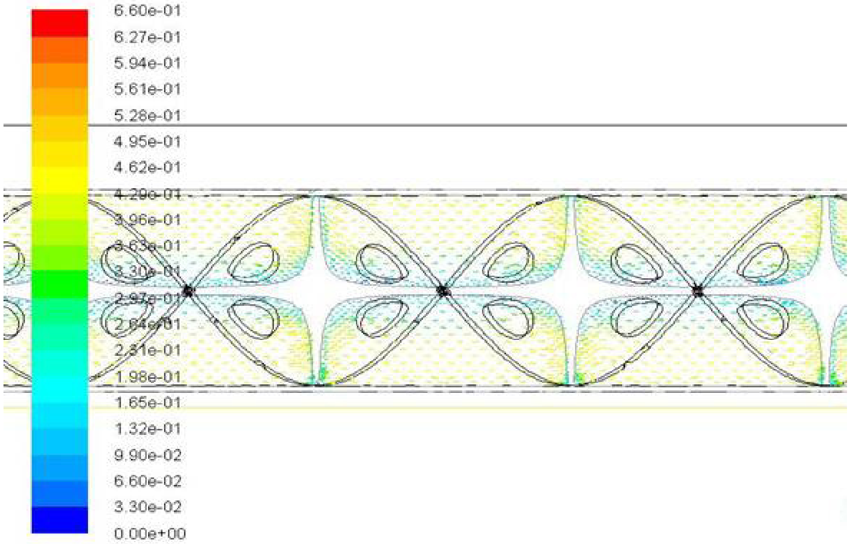

Figure 12. Side view of velocity vectors in a plane of augmented pipe with parallel circular perforated twisted tape.

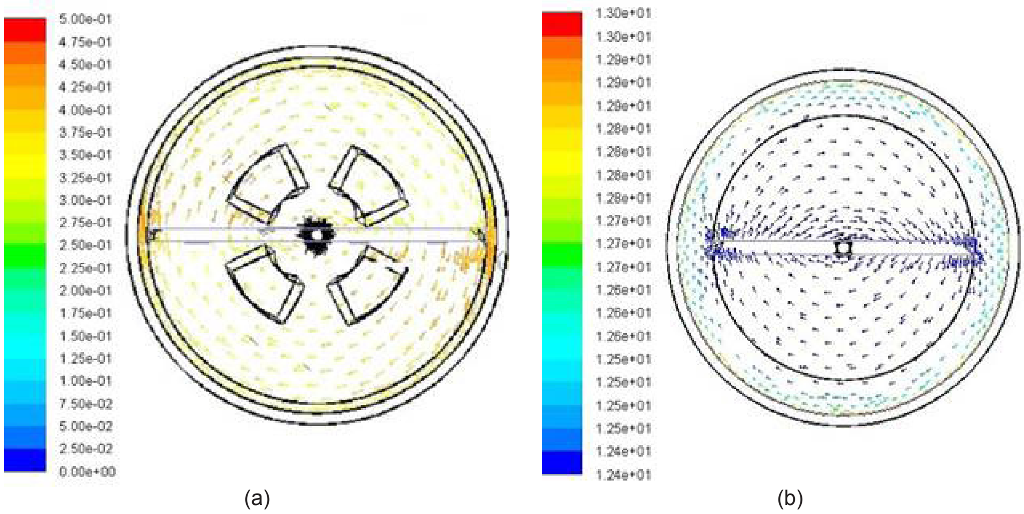

Figure 13. Front view of (a) velocity vector plot (in m/s) of a parallel rectangular perforated twisted tape and (b) temperature profile of single twisted tape (in °C) of a plane, 0.9m away from the inlet.

the temperature of the water is maximum near to the pipe wall, and it decreases towards the center of the pipe. The temperature along with the direction of flow can be seen in this plot. Some portion of the temperature profile near the pipe can be seen in yellow colour stating that temperature is high in these areas as the temperature at the pipe is high. As these results are only for 1.8 m length of the pipe, the computational results show a temperature decrease of 7 °C across the whole confined space.

We have experimentally passed water into the pipe at an inlet temperature of 12.4 °C. Figure 14 shows the temperature distribution from the floor surface to the pipe interiors. The temperature outside the pipe surface, i.e. at the interface of pipe and concrete is around 25 °C, and the highest temperature of 42°C is seen at the surface of the floor of our confined space from Figure 1. Due to symmetrical boundary conditions applied on both sides of the pipe, the temperature is distributed according to the symmetry wall boundary.

For steady-state, after the convergence, the mass flow rate at the inlet and outlet of air and water was achieved to be the same due to the same surface area of water inlet and outlet. The mass flow rate of water is 0.58 kg/s.

Figure 15 shows the velocity magnitude path lines of a pipe augmented with twisted tapes having a constant twist ratio. We can observe from the figure that lines at the pipe

J Ther Eng, Vol. 7, No. 7, pp. 1614–1627, November, 2021

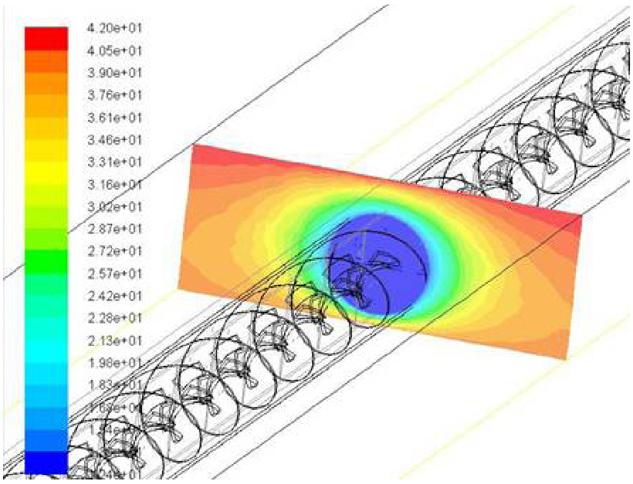

Figure 14. Temperature contour showing temperature distribution in a normal plane of a pipe augmented with a twisted tape having a constant twist ratio at the pipe inlet from the floor surface to the pipe interior.

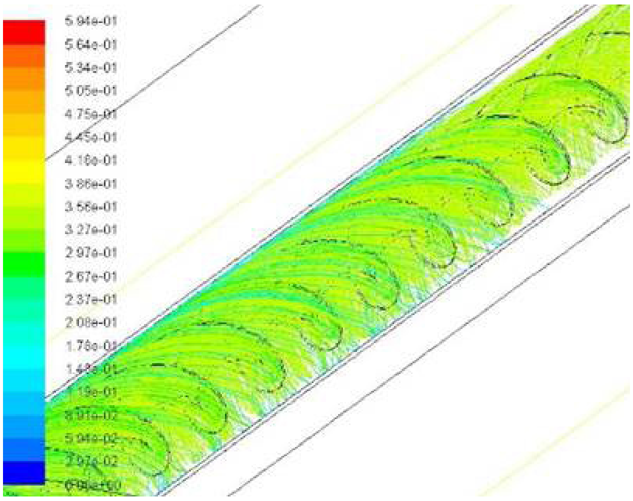

Figure 15. Isometric view of path lines of a twisted pipe showing velocity magnitude.

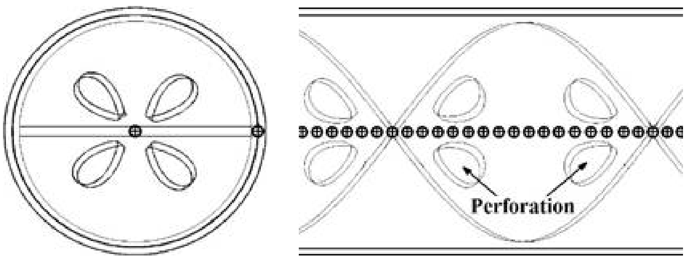

Figure 16. Rake positions inside the pipe inserted with parallel circular perforated twisted tape.

inner boundary show green colour and lines at inside the boundary show yellow colour stating that the velocity magnitude is less near the boundary and high going from surface to the centre due to no-slip condition as blue colour is seen at the surface.

RESULTS AND DISCUSSION

To obtain results, a set of points (rakes) have been inserted from inlet to outlet with an interval of 0.01 m to get the absolute values of temperature at these points. For a detailed study, two sets of points in all cases are at the center of the pipe and near to floor surface in a fluid cell zone are studied.

From Figure 16, rake positions inside the pipe of parallel circular perforated twisted tape are used to get the absolute temperature. The graph of temperature taken from the axis of pipe in Kelvin with length from inlet to outlet in the meter is plotted and shown in Figure 17.

Absolute temperature from inlet to outlet increases because water gains heat from the floor surface through the concrete and pipe wall. The floor gets cooled down, as shown in the graph of temperature taken from the top axis of pipe with length from inlet to outlet in Figure 17. The mass flow rate and velocity of water are almost considered to be constant for all the cases. The heat removal takes place predominantly due to fluid swirl flow. The maximum amount of heat removal takes place in the twisted tape with an increasing twist ratio. The readings for steady-state conditions were taken for water inlet and water outlet after convergence was achieved.

Figure 17 shows the graph of temperature values of the simulation of ANSYS-FLUENT obtained along the length of the pipe. The inlet water temperature is 12.55 °C. From Figure 17, we can see that maximum cooling of the floor surface and heat transfer enhancement occurs in the case of twisted tape with an increasing twisted ratio. The temperature goes from 285.55 K to 286.83 K. Initially the slope starts decreasing after which it increases. After this, heat enhancement can be seen in the following decreasing order: parallel circular perforated twisted tape, double zigzag circular perforated TT, double parallel slotted TT, zigzag rectangular perforated TT, double zigzag rectangular perforated TT, double zigzag slotted TT. After this sequence,

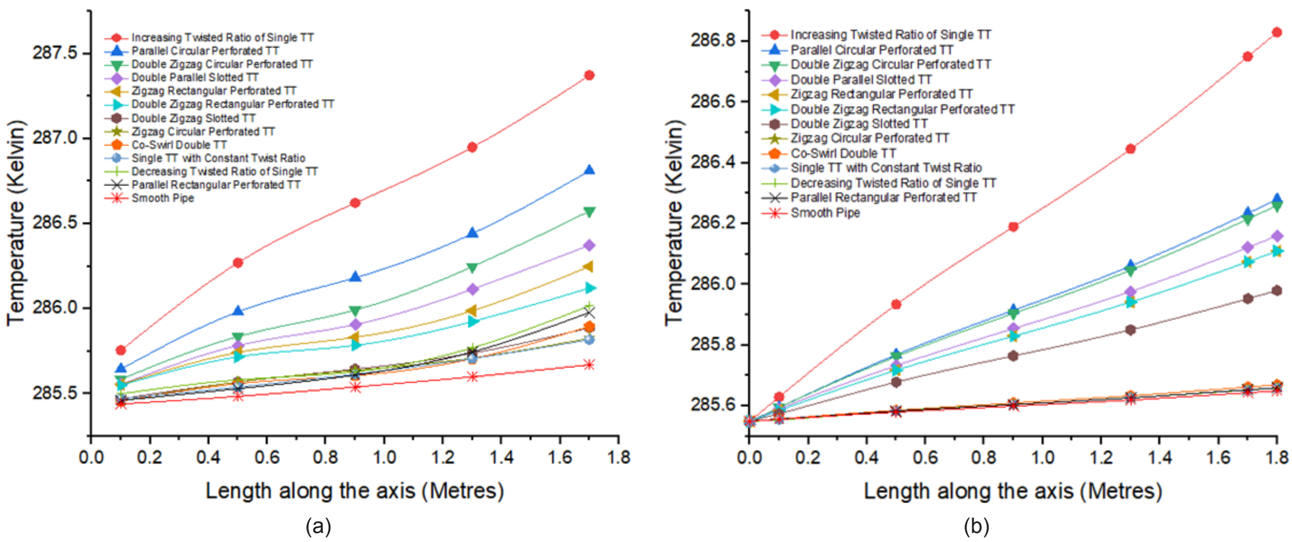

Figure 17. Graph of (a) experimental and (b) simulation data taken along offset to the axis of the pipe.

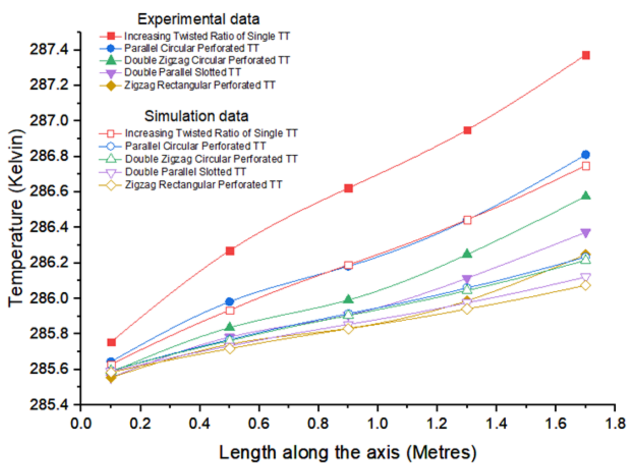

Figure 18. Comparison between the experimental and numerical values.

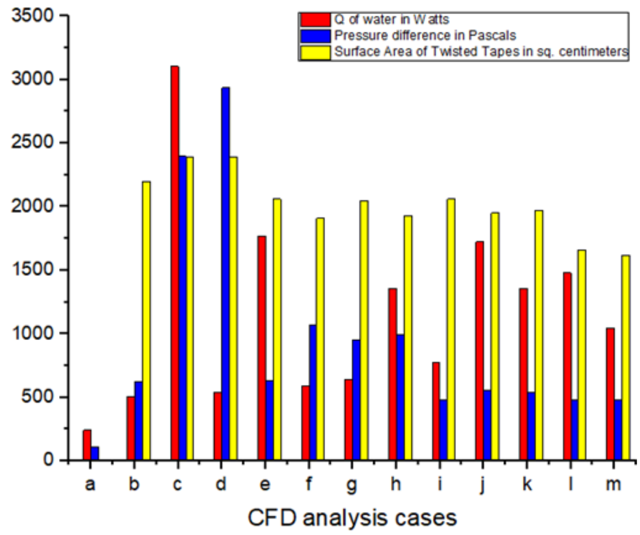

Figure 19. Bar chart of CFD analysis cases with heat removed, pressure change and surface area of TT.

we can observe the overlapping of temperature values. As expected, lowest heat transfer is obtained in the case of a smooth pipe as it has no inserts for swirl flow and turbulence and thus less heat transfer coefficient.

We have performed experiments corresponding to all the 13 twisted tape configurations. The inlet temperature was kept constant to 12.4 °C and temperatures were noted using thermocouples. Cold water tank temperature was fixed accordingly so that inlet temperature. During the experiment, we found that the inlet water temperature was fluctuating and in the range of 12.24 °C to 12.7 °C due to external errors. The highest value at 1.7 m was obtained for TT with increasing twisted ratio, which is 287.37 K. This was 0.62 K higher than simulation value. The result was in order with the simulation result. A constant pressure pump was used in the experiments. As the twist ratio increases, higher pressure and thus lower velocity values are obtained going from inlet to outlet and the turbulence is increased. This increases the residence time of water with the pipe wall and thus higher heat transfer. In the case of decreasing twist ratio, low pressure and high velocity is observed at the outlet compared to the inlet. Thus, a lesser heat is transferred in case of TT with decreasing twist ratio compared to TT with increasing twist ratio.

We can observe the same trend as shown above till double zigzag rectangular perforated twisted tape after which the twisted tape with decreasing twisted ratio and parallel rectangular perforated TT saw a sudden increase. The order was mixed up later on. As expected, the smooth pipe without any insert inserted saw a minimum temperature difference between inlet and outlet. It showed a difference of 0.06 K between experimental and simulation value at 1.7 m. Twisted tape with constant twist ratio was just above smooth pipe in terms of temperature difference in both experimental and simulation sections. We can observe a significant gap between the smooth pipe and single TT with constant twist ratio in the experimental section which is not observed in simulation values which have very less difference. The steady-state conditions were analyzed for smooth and augmented pipe and the following results were obtained. Comparing the heat transfer coefficient between the fluid and the wall, we get a value of 0.11 W/m^{2}K for twisted tape with decreasing twist ratio and 0.25 W/m^{2}K for TT with parallel circular perforation.

Figure 18 shows the comparison of experimental and simulation data in a single graph.

From the above Figure 19, we observe that the maximum amount of heat is being removed from the twisted tape with increasing twist ratio. The highest-pressure difference is observed in case of twisted tape with decreasing twist ratio followed by twisted tape with increasing twist ratio. For smooth pipe, both the heat transfer and pressure difference are very low compared to other augmented pipes. The surface areas of twisted tape are taken to be almost constant. We find a small difference in the surface areas of twisted tapes due to the orientation and perforations in the tapes. Twisted tape with increasing and decreasing twist ratio has the highest surface area of twisted tapes which is equal to 0.239 cm^2. The Pressure drop for increasing and decreasing twisted tape is more than twice of all other cases. In augmented pipes, the lowest pressure change is observed in the case of double parallel slotted TT.

There are various reasons for the deviation of experimental values from simulation values. The experimental and simulation data varies due to non-uniform meshing elements, friction factor change due to reduction in temperature difference along the length, difficulty in maintaining symmetric boundary conditions during the experiment and change in ambient temperature while performing experiments. In the simulation, a smooth pipe is considered, but in reality, some roughness is always present. Uniform heating is considered, which might not occur in practical cases. Thermocouple temperature detection error, varying of actual mass flow rate due to inaccurate pumping of cold water, movement of twisted tapes due to water flow inside the pipe, inaccurate and non-uniform twist ratio in practical cases are some of the errors due to which deviation occurs.

CONCLUSION

After the analysis of thirteen cases of smooth and augmented pipes, it was found that twisted tape with increasing twist ratio was the most efficient one for heat transfer enhancement. It removes maximum heat from the confined space than others because it has 8.64% more surface contact with water compared to twisted tape with constant twist ratio, and the intensity of swirl flow increases from inlet to outlet. It is 12.8 times efficient than smooth pipe without inserts and 6.09 times efficient than an augmented pipe with a twisted tape of constant twist ratio in terms of heat transfer. It is 75.34% more efficient than parallel circular perforated twisted tape. In practice, it is difficult to work for the pump to create that much pressure accurately in case of single twist tape with decreasing twist ratio. Out of these, the twisted tape with an increasing twist ratio should be used in the pipe for the most heat transfer enhancement. A temperature difference of 1.618 ^{o}C for water was observed for this case for a length of 1.8 meters. Laying the pipe across the whole room gave a temperature reduction of 7 ^{o}C from the simulation results. Similarly, the parallel circular perforated and the double zigzag circular perforated twisted tapes gave a temperature difference of 1.166 ^{o}C and 0.99 ^{o}C respectively. From this study, the heat transfer is being enhanced from all augmented cases. In the co-swirl double twisted tapes, the swirl flow created is 50% less than single twisted tape. The double zigzag rectangular perforated twisted tapes are studied it was found that it is 30.23% better as compared to the zigzag slotted with double twisted tape. Also, due to parallel rectangular perforations, it enhances swirl flow and creates more turbulence. Experimental data was in order with simulation data for six of the initial cases after which overlapping was observed. Lowest heat transfer enhancement was observed in twisted tape with constant twist ratio in augmented pipes. The surface roughness and friction factor of the twisted tape is also an important factor to decide heat transfer improvement.

NOMENCLATURE

A	Surface area of the pipe, m^2
C_{pf}	Specific heat of fluid, kJ / kg ^{o}C
k	Thermal conductivity, W / m ^{o}C
Q	Heat transfer rate, W
$\dot{m}$	Mass flow rate, kg/s
f	Friction factor
h	Heat transfer coefficient, W / m^2 ^{o}C
T	Temperature, ^{o}C
T_f	Inlet temperature of the fluid, ^{o}C
u_f	Inlet velocity of the fluid, m/sec
t	Thickness of twisted tape
TT	Twisted Tape

Greek symbols

θ	Twist angle measured from a side view, rad
ρ_f	Density of a fluid. kg/m^3

Subscripts

f	Refers to fluid
a	Augmented
s	Smooth

Dimensionless parameters

Re Reynolds number = ρvd/μ
Nu Nusselt number = hl/k

AUTHORSHIP CONTRIBUTIONS

Authors equally contributed to this work.

DATA AVAILABILITY STATEMENT

The authors confirm that the data that supports the findings of this study are available within the article. Raw data that support the finding of this study are available from the corresponding author, upon reasonable request.

CONFLICT OF INTEREST

The author declared no potential conflicts of interest with respect to the research, authorship, and/or publication of this article.

ETHICS

There are no ethical issues with the publication of this manuscript.

REFERENCES

[1] Eiamsa-ard P, Piriyarungroj N, Thianpong C, Eiamsa-ard S. A case study on thermal performance assessment of a heat exchanger tube equipped with regularly-spaced twisted tapes as swirl generators. Case Stud Therm Eng 2014;3:86–102. [CrossRef]

[2] Maradiya C, Vadher J, Agarwal R. The heat transfer enhancement techniques and their thermal performance factor. Beni-Suef Uni J Basic Appl Sci 2017;7:1–21. [CrossRef]

[3] Tamna S, Kaewkohkiat Y, Skullong S, Promvonge P. Heat transfer enhancement in tubular heat exchanger with double V-ribbed twisted-tapes. Case Stud Therm Eng 2016;7:14–24. [CrossRef]

[4] El Maakoul, A, Laknizi A, Saadeddine S, Ben Abdellaha A, Mezianec M, El Metouiet M. Numerical design and investigation of heat transfer enhancement and performance for an annulus with continuous helical baffles in a double-pipe heat exchanger. Energy Convers Manage 2017;133:76–86. [CrossRef]

[5] Yongsiri K, Eiamsa-ard P, Wongcharee K, Eiamsa-ard S. Augmented heat transfer in a turbulent channel flow with inclined detached-ribs. Case Stud Therm Eng 2014;3:1–10. [CrossRef]

[6] Murugesan P, Mayilsamy K, Suresh S. Heat transfer in tubes fitted with trapezoidal-cut and plain twisted tape inserts. Chem Eng Commun 2011;198:886-904. [CrossRef]

[7] Deshmukh P, Vedula R. Heat transfer and friction factor characteristics of turbulent flow through a circular tube fitted with vortex generator inserts. Int J Heat Mass Transf 2014;79:551–560. [CrossRef]

[8] Promvonge P, Skullong S, Kwankaomeng S, Thiangpong C. Heat transfer in square duct fitted diagonally with angle-finned tape—part 1: experimental study. Int Commun Heat Mass Transf 2012;39:617–624. [CrossRef]

[9] Skullong S, Thianpong C, Jayranaiwachira N, Promvonge P. Experimental and numerical heat transfer investigation in turbulent square-duct flow through oblique horseshoe baffles. Chem Eng Process 2016;99:58–71. [CrossRef]

[10] Sivashanmugam P, Nagarajan P, Suresh S. Experimental studies on heat transfer and friction factor characteristics of turbulent flow through a circular tube fitted with right and left helical screw-tape inserts. Chem Eng Commun 2008;195:977–987. [CrossRef]

[11] Chang S, Gao J, Shih H. Thermal performances of turbulent tubular flows enhanced by ribbed and grooved wire coils. Int J Heat Mass Transf 2015;90:1109–1124. [CrossRef]

[12] Skullong S, Kwankaomeng S, Thianpong C, Promvonge P. Thermal performance of turbulent flow in a solar air heater channel with rib-groove turbulators. Int Commun Heat Mass Transf 2014;50:34–43. [CrossRef]

[13] Bhuiya M, Chowdhury M, Shahabuddin M, Saha M, Memon L. Thermal characteristics in a heat exchanger tube fitted with triple twisted tape inserts. Int Commun Heat Mass Transf 2013;48:124–132. [CrossRef]

[14] Date A, Saha S. Numerical prediction of laminar flow and heat transfer characteristics in a tube fitted with regularly spaced twisted-tape elements. Int J Heat Fluid Flow 1990;11:346–354. [CrossRef]

[15] Xu X, Wang S, Wang J, Xiao F. Active pipe-embedded structures in buildings for utilizing low-grade energy sources: a review. Energy Build 2010;42:1567–1581. [CrossRef]